Accuracy Investigation of the Orthorectification Strategies for High Resolution Satellite Images

By

Prof. Dr. Ahmed A. Shaker — **Assoc. Prof. Ali A. ElSagheer**
Dr. Ayman R. ElShehaby — **Eng. Mahmoud S. Mahmoud**

Department of Surveying Engineering, Shoubra Faculty of Engineering, Zagazig University.

ملخص البحث

تسبب الخرائط القديمة العديد من المشاكل للمهندسين والمخططين وغيرهم ممن يحتاجون إلى تخطيط أعمالهم بدقة ويحتاجون دائماً إلى خرائط حديثة ومتطورة بقدر الإمكان. وللتغلب علي هذه المشكلة فإنه يجب تحديث الخرائط المتاحة وذلك يتطلب إما إلي مراجعة أرضية تقليدية مكثفة للخرائط المتاحة مما يتطلب الكثير من الوقت والجهد والتكلفة أو استخدام الصور الجوية لهذا الغرض وهذا يحتاج إلى تكلفة عالية بالإضافة إلى تصاريح روتينية يصعب توافرها في كثير من الأحيان. لذلك يهدف هذا البحث بشكل رئيسي إلى وضع آلية لتحديث الخرائط ذات مقاييس الرسم الكبيرة بالاستعانة بصور الأقمار الصناعية عالية الدقة وذلك من خلال تقويم هذه الصور رأسياً بإتباع عدة طرق رياضية مختلفة، مع الأخذ في الاعتبار الإزاحة الناتجة عن تضاريس سطح الأرض كذلك الإزاحة الناتجة عن ارتفاعات المباني. وللوصول إلي ذلك تم إجراء عدة تجارب معتمدة علي نوعين من نقاط التحكم: أولاً باستخدام إحداثيات نقاط تحكم أرضية (GCPs) مرصودة بنظام الـ GPS، ثانياً باستخدام إحداثيات لنقاط دليليه مقاسه من الخريطة نفسها (MRPs). وفى كلتا الحالتين تم استخدام العديد من النماذج الرياضية كما تم دراسة تأثير نموذج سطح الأرض الرقمي (DEM) وكذلك نموذج المباني الرقمي (DBM) الذين تم تخليقهما خصيصاً لهذا الغرض بمنطقة الدراسة. و سجلت نتائج هذه التجارب وتم تحليل النتائج التي أظهرت الأهمية القصوى لاعتبار تضاريس سطح الأرض وكذلك ارتفاعات المباني ومدي تأثيرها الواضح علي دقة الإحداثيات المنتجة وبالتالي علي عملية تحديث وإنتاج الخرائط من صور الأقمار الصناعية عالية الدقة والمقومة رأسياً.

ABSTRACT

Obsolete maps creates so many problems to engineers, planners and other professionals who need to develop there work based on updated records. The conventional methods of map revision with traditional surveying techniques and aerial photographs are costly and time-consuming. The main objective of this research is to investigate the accuracy of the Orthorectification strategies for High Resolution Satellite Images (HRSI) for producing Ortho-Maps and setting up a workflow for updating large-scale maps utilizing high-resolution satellite imagery. In order to achieve Orthorectified satellite image, two experiments were conducted to evaluate the planimetric accuracy for the produced Ortho-Map: the first one based on Ground Control Points (GCPs) observed using Global Positioning System

technology (GPS); the second one based on Map Reference Points (MRP) measured directly from the digital base map. Also the effect of using both created Digital Elevation Model (DEM) and Digital Building Model (DBM) on the Orthorectification process was evaluated. Finally, the used models are specified and the obtained results are tabulated and analyzed. From the obtained results; available cadastral data (1:5,000 map) with MRPs, DEM and DBM are sufficient for orthorectifying the IKONOS image with the accuracy of the 1:10,000 base map. Also, by using the available GCPs, the same DEM and DBM are sufficient for orthorectifying the IKONOS image with the accuracy of the 1:5,000 base map.

1. Introduction

Maps are essential database for both planning and fieldwork operation. Up-to-date maps are necessary because obsolete maps create so many problems to engineers, planners and other professionals. On the other hand most developing countries have great difficulties in systematic updating of their maps. In addition to the fact that large areas of such countries are not mapped, many of the existing maps are old and sometimes have unsuitable scale. The conventional methods of map revision with aerial photographs are costly and time-consuming that base map revision cycle cannot be done as planned. However, the recent availability of high-resolution satellite data such as SPOT, IKONOS, QUICKBIRD offer an interesting alternative for map production and updating [Somkiat, 1990]. Space imagery promises to be will appropriate to produce and update maps. It would be an attractive solution to such countries whose mapping needs are difficult to satisfy using aerial photogrammetric techniques [Ridley, et. al., 1997]. Thus, it becomes crucial to develop unconventional strategies for map updating. The main objective of this research is to investigate the accuracy of the Orthorectification strategies for high resolution satellite images for producing Ortho-Maps and setting up the workflow, given in Figure (1), for updating large-scale maps utilizing high-resolution satellite imagery HRSI.

2. Study Area and Available Data

The area of study is selected at Sakr-Korish area, Al Madii, Cairo City. The area is approximately one and half km^2. It is a largely urban area that contains buildings, a network of main roads as will as minor roads and some hilly areas. The following data sources are available for the study area:

- A one-meter spatial resolution, panchromatic image over the area of study was collected in April 17, 2000 by Space Imaging's IKONOS satellite and supplied in a

TIFF digital format. This image has been radiometrically corrected to improve the radiometric quality by the producer, Figure (2).

- A 1:5000 Cadastral map (J-17) of the same area of study produced in 1978 from 1:15000 aerial photographs acquired in 1977 (IGN Series), Figure (3). The map is published by the Egyptian Survey Authority (ESA), projected into the Universal Transverse Mercator projection (UTM).
- A 1:5000 Topographic map over the same area produced in 1978 from the same aerial photographs is used for generating the (DEM) digital elevation model required for the orthorectification process, Figure (4). The map is published by the Egyptian Survey Authority (ESA), projected into the Universal Transverse Mercator projection (UTM).

3. Map Vectorization and Georeferencing

Scanning is a very common procedure used for transforming hard copy maps into a digital format, where the output is a raster map [Smith, et. al., 1999]. Scanners come in three general types: line-following scanners, flatbed scanners and drum scanners [Michael, 1999]. Experience has shown that a resolution of 400 to 600 D.P.I (Dots Per Inch) gives the best scanning results. This resolution avoids line coalescence while still resolving very thin lines that might not be totally captured at lower resolutions, also this resolution will prevent most difficulties at the vectorization step [Thomas and Ralph, 2000]. The 1:5000 hard-copy cadastral map has been scanned using Acer-A0 flatbed scanner at a resolution of 100 microns (250 dpi). That corresponds to a ground pixel size of 50.8 cm, which is consistent with the planimetric accuracy of the 1:5000 scale map and also with the spatial resolution of the used IKONOS image.

After that a process involves the conversion of data in analog form into a digital form that is directly readable by a computer, vectorization, should be performed. This is normally achieved manually by a human operator using a digitizer, although methods of automated vectorization and semi-automated vectorization also exist. The result of digitizing is a digital map in vector form [Eileen, 1998]. In this research, and due to the limitation of automatic vectorization software on hand, the scanned map had been imported into the ERDAS IMAGINE 8.4 environment [Erdas, 1997] and vectorized using on screen digitizing approach, Figure (5).

The process involved georeferencing of both scanned and vectorized maps to the Universal Transverse Mercator projection (UTM) by the map corners coordinates in the ERDAS IMAGINE 8.4 software. To evaluate the planimetric accuracy of the map nearly 25 ground control points (GCPs) evenly distributed through the area of study and well defined on both the map and ground were selected. GPS observations were carried out and compared against the corresponding map reference points (MRPs), Table (1). All points were results in the UTM (Universal Transverse Mercator) system as previously mentioned.

4. Generation of the Digital Elevation Model (DEM)

To generate the DEM to be used for the orthorectification process the 1:5000 topographic map mentioned before was scanned, then georeferenced to the Universal Transverse Mercator projection (UTM) projection and a raster to vector conversion process (on-screen digitizing) was used (nearly 26342 point were digitized). The contour lines vector data were compiled by adding elevation attributes, and the DEM was built from the vector data by ERDAS IMAGINE 8.4 software, Figure (6). The terrain for the study area varies from 45 m up to 115m above Mean Sea Level (M.S.L). For practical estimates and tests the DEM accuracy, ordinary leveling from Bench Mark No. (8144) of level 53.741m above men sea level have been done for 15 check points evenly distributed across the area of interest. Table (2) illustrate the DEM interpolated heights, leveling heights and the height differences for these checkpoints.

5. Generation of the Digital Building Model (DBM)

High quality and homogenous Digital Building Model (DBM) can be directly derived from Airborne Laser Scanner (ALS) data. Airborne laser scanner is an active technique to acquire 3D information describing the earth surface. A typical system can provide pixel data with 15cm vertical accuracy and 50cm horizontal accuracy, and the laser points are almost evenly distributed in the covered area [Guo and Yasuoka, 2001]. Unfortunately, there is no ALS data over our area of interest, so the Digital Building Model (DBM) had been generated manually, where the positions of Buildings were digitized from the scanned map in the ERDAS EMAGINE 8.4 environment using on-screen digitizing technique for the area of interest. The elevation data were measured

using the remote elevation program in the SOKKIA SET3000 Total Station and compiled by adding elevation attributes, where the building heights range from 3m to 33m. After that all the areas in between had been masked to the datum level, Figure (7).

6. Rectification of Satellite Imagery

To make the satellite imagery useful for mapping or map updating, the imagery must be adjusted to a geographic map projection. This process is often called georeferencing. It converts the image from an arbitrary coordinate system into that of the applied map source [Smith, et. al., 1999]. Two main processes within rectification warrant further explanation:

6.1.Coordinate Transformation

There are a variety of transformation models, but here we applied the most commonly used ones in image processing systems. In the following sub-sections the used transformation models in this investigation are discussed briefly.

6.1.1 Polynomials Transformation Model

The transformation between the original and the rectified images is done by polynomial models, that is [Shaker, et. al., 2002]:

$$fx(x', y') = x = x^{\pi} A\, y' \quad (1)$$

$$fy(x', y') = y = x^{\pi} B\, y' \quad (2)$$

where

x , y are coordinates of the original image,

x', y' are coordinates of the rectification,

A, B are coefficient matrices of the polynomials;

$x^{\pi} = (1, x'_1, x'_2, x'_3, \ldots)$

$y^{\pi} = (1, y'_1, y'_2, y_3, \ldots)$

This method corrects for distortions of the image relative to a dense set of control points. Due to the polynomial transform, the original image is shifted, rotated, scaled, and squeezed so that it fits well to the given reference points. A first order (linear) transformation can change location, scale, skew and rotation. Second order transformations can correct nonlinear distortions. They can be used with data covering a

large area to account for the Earth's curvature and with distorted data (for example, due to camera lens distortion). Third order transformations can be used with distorted aerial photographs and with radar imagery. Fourth order transformations are suitable for very distorted aerial photographs [Erdas, 1997].

6.1.2 Rubber Sheeting Transformation Model

Rubber Sheeting transformations reconstruct the digital images in "patches" between ground control points (GCPs). These patches are typically triangles that form an irregular mesh covering most or the entire image. The transformation of the image is then executed on a triangle by triangle basis. A GCP exerts influence only on those triangles in which it is a vertex. While each triangle will have a different transformation function, adjacent triangles will share the same transformation function values at their common edge. This makes the piecewise transformation continuous across the image so that the transition from one triangle to another becomes seamless. Suppose a triangle has vertices P_1, P_2, P_3 with corresponding image space coordinates of (u_1,v_1), (u_2,v_2), (u_3,v_3) and target space coordinates (x_1,y_1), (x_2,y_2), (x_3,y_3). For a point P within the triangle, with target space coordinate (x,y), the corresponding image space coordinate (u,v) is found by solving [Smith, et. al., 1999]:

$$x = Ar \tag{3}$$

$$u = Br \tag{4}$$

where:

$$r = \begin{vmatrix} r1 \\ r2 \\ r3 \end{vmatrix} \quad A = \begin{vmatrix} x1 & x2 & x3 \\ y1 & y2 & y3 \\ 1 & 1 & 1 \end{vmatrix} \quad X = \begin{vmatrix} x \\ y \\ 1 \end{vmatrix} \quad U = \begin{vmatrix} u \\ v \end{vmatrix} \quad B = \begin{vmatrix} u1 & u2 & u3 \\ v1 & v2 & v3 \end{vmatrix}$$

Once the transformation equation has been solved an interpolation method is used to determine an output intensity value.

6.1.3 Differential Transformation Model

A digital elevation model (DEM) is needed to correct for relief displacements in the image. The three dimensional coordinates (x, y, z) defined by a DEM pixel are transformed into the image by the Collinearity Equations (5) and (6). At the image

position (x, y) the gray-value is interpolated by one of the resampling methods. The density is stored at the x, y location of the digital orthophoto, which is equal to the position of the DEM point [Shaker, et. al., 2002]:

$$x = xp - c\frac{r11(Xo - Xo) + r21(Y - Yo) + r31(Z - Z0)}{r13(X - Xo) + r23(Y - Yo) + r33(Z - Zo)} = fx(x`, y`) \quad \text{.....(5)}$$

$$y = yp - c\frac{r11(X - Xo) + r21(Y - Yo) + r33(Z - Z0)}{r13(X - Xo) + r23(Y - Yo) + r33(Z - Z0)} = fx(x`, y`) \quad \text{.....(6)}$$

where x', y' are equivalent to the map coordinates x, y.

To perform this transformation, the following parameters have to be available:

- The interior orientation of the camera: xp, yp, c.
- The exterior orientation of the camera: Xo, Yo, Zo
- Perspective center, R a rotation matrix composed of ω, φ, κ rotation angles,
- The pixel spacing of the digital image in camera units: px, py (mm).
- The cell-size of the DEM pixels in ground units: gx, gy. (m).
- The reference coordinates of one DEM pixel in the given map projection (usually the left upper corner of the DEM file).

6.2 Resampling

The row and column coordinates from the transformation process are not integer values. Since the satellite image has digital numbers only for integral locations, a procedure is required to obtain the proper value from the satellite image. This procedure is commonly called resampling [Smith, et. al., 1999]. There are several techniques available for resampling of digital images, through three particulars ones are by the most prevalent. These three are known as Nearest Neighbor interpolation, Bilinear interpolation and Bicubic interpolation [Moik, 1980].

7. Methodology of Investigation and Discussion of the Obtained Results

Two different approaches are investigated for the orthorectification of the satellite images. These approaches are:

a. The first approach based on ground control points (GCPs) are obtained by GPS technology and the generated Digital Elevation Model (DEM) with a grid size of 5m from the available 1: 5,000 topographic map.

b. The second approach based on Map Reference Points (MRPs), derived from the available 1:5,000 Cadastral map and the generated Digital Elevation Model (DEM) with a grid size of 5m from the available 1: 5,000 topographic map.

In this context, several strategies and mathematical models are applied and the following results are obtained:

- For GCPs control points several mathematical models and control point configurations were applied and the results were recorded in Table (3) and graphically represented by Figure (8).
- Also for MRPs several mathematical models and control point configurations were applied and the results were recorded in Tables (4) and graphically represented by Figure (9).
- The effect of DBM on the orthorectification process in both cases of control points was tested and the results are recorded in Tables (5) and (6) respectively.
- Also the effect of the error in measuring building heights on the horizontal position of the building were discussed and represented numerically in Table (7) and graphically in Figure (10).

The finals obtained results are:

- The palnimetric accuracy of the map georeferencing is 1.825m.
- The generated DEM have standard error of the elevation is 1.167m.
- The generated orthoimage, by using DEM and by considering building effects DBM may reach an accuracy of 1.838m when 10 MRPs were employed.
- The generated orthoimage, by using DEM and by considering building effects DBM may reach an accuracy of 0.838m, when 10 GCPs were employed.
- The large RMSE of image registration using map MRPs may be due to some problems with the existing map, which we used for GCPs collection. It may have

some paper distortions or some errors during the process of scanning and raster-to-vector conversion.

- The quality of the orthorectification process was examined on the screen by overlaying satellite images with the digitized vector map. The most accurate terrain features are the roads. They were coincide within one or two meter since the image has already orthorectified using the digital elevation model (DEM). While the planimetric positions of buildings were still dislocalized by relief displacement comes from the buildings so, a Digital Building Model (DBM) is necessary.

8. Concluding Remarks

In this research, accuracy investigation of the orthorectification strategies for high-resolution satellite images for producing Ortho-Maps was performed. Two different approaches are investigated, GCPs and MRPs, for the orthorectification of the satellite images. Also, the potential of both DEM, DBM on the orthorectification process is evaluated. Based on the obtained results, the following concluding remarks can be made:

- Using available planimetric data from 1:5,000 Cadastral maps as MRPs and a Digital Elevation Model (DEM) with a grid size of 5m are sufficient for orthorectifying the IKONOS image with the accuracy of the 1:10,000 base map.
- Using available GCPs and the same Digital Elevation Model (DEM) with a grid size of 5m were sufficient for orthorectifying the IKONOS image with the accuracy of the 1:5,000 base map.
- In flat areas, geometric correction can be implemented by transformation of planimetric control points (simple rectification). While in hilly areas, relief displacement by terrain variation are significant and should be compensated so a 3-dimensional transformation should be used and (orthorectification) with DEM.
- Also, the potential of DBM on the orthorectification process is significant in the flat and hilly areas.
- The technology based on high-resolution satellite imagery will be of suitable cost and time effective for updating old maps at large and medium scales.

- The time and cost required to producing a 1:5000 Ortho-phot map (2.5 X 3.5 Km) from 1m panchromatic IKONOS imagery may be reduced by 5.5 times than the traditional techniques.
- The resulting maps provide useful information that is necessary for planning and decision making at national and regional levels.
- Generally speaking, the use of IKONOS data for change detection of land cover and land use at scale of 1:5000 led to good results. However, their spatial resolution was always sufficient to interpret the individual classes clearly.

References

Eileen, M., (1998): "Planning a Digitizing Project.", the NVGIA GIS, Core Curriculum for Technical Programs, October 5, 1998.

Erdas, (1997): "Imagine Essentials Training Reference Manual.", Atlanta, Georgia, USA.

Guo T. and Yasuoka Y., (2001): "Combining High Resolution Satellite Imagery and Airborne Laser Scanning Data for Generating Bareland DEM in Urban Areas.", International Archives of Photogrammetry, Remote Sensing and Spatial Information Science, Kumming, China, ISSN.

Michael N., (1999): "Fundamentals Of Geographic Information Systems.", Second Edition, New Mexico, State University.

Moik, J., (1980): "Digital Processing of Remotely Sensed Images.", NASA SP-431, Washington, D.C., Government Printing Office.

Ridley, H., Kinson, P., Alpin, P., Muller, J., and Dowman, I., (1997): " Evaluating the Potential of the Forthcoming Commercial U.S. High Resolution Satellite Imagery as the Ordnance Survey.", PE&RS, Vol. 63, No. 8.

Shaker, A., Zahran, M., and ElSagheer, A.,(2002): " A Proposed Approach to Update Large-Scale Maps in Developing Countries Using High-Resolution Satellite Imagery.", Civil Engineering Research Magazine, Al Azhar University, Vol. 24, No. 1 Jun. 2002. Page 344-362.

Smith,S., Dewitt, B., Gonzalez, E., and Hurt, G., (1999): " Georeferencing of Satellite Imagery for Digital Soil Mapping.", Surveying and Land Information System.Vol.55, No.1, PP.13-20.

Somkiat, A., (1990): "Base Map Revision Using High Resolution Satellite Data.", Royal Thai Survey Department, Thailand.

Thomas, M., and Ralph, W., (2000): "Remote Sensing and Image Interpretation.", Fourth Edition.

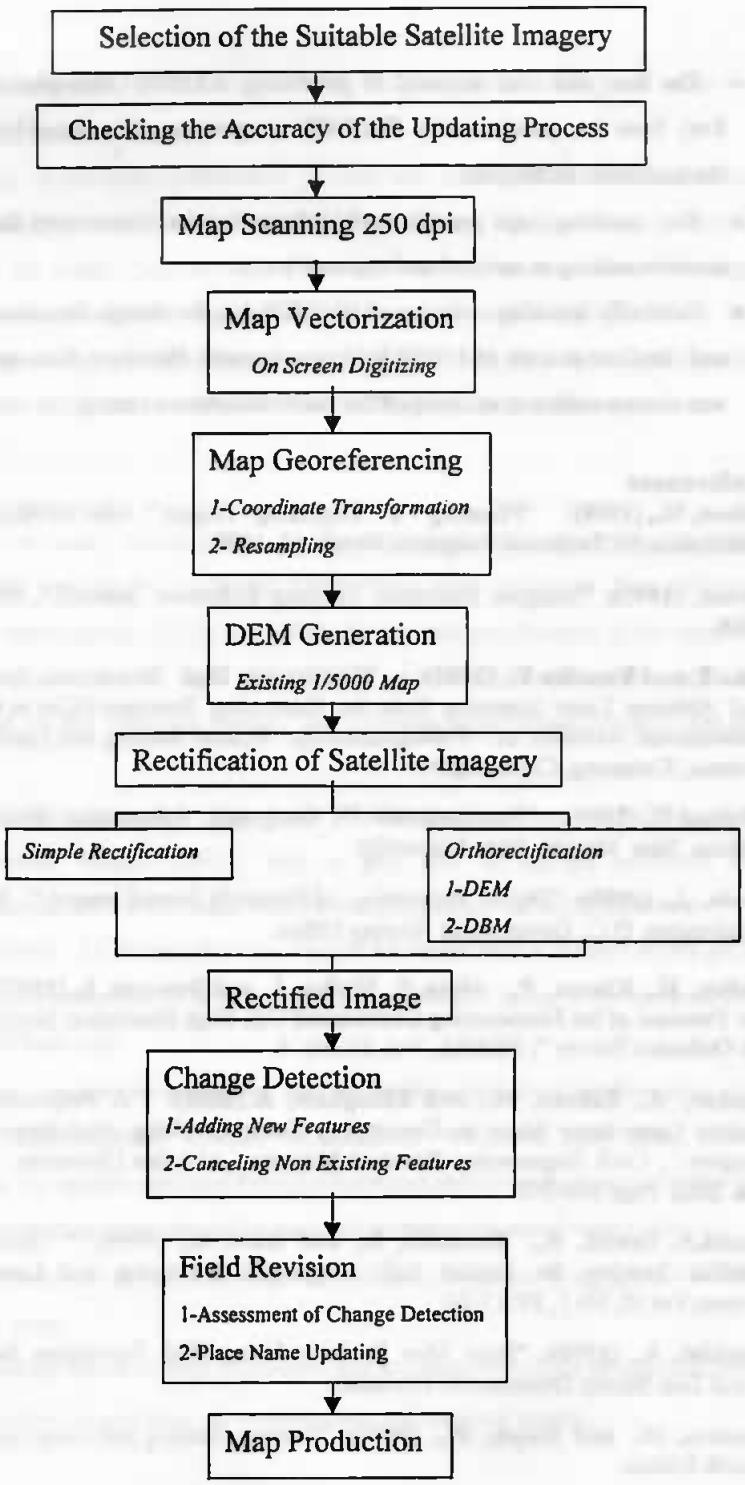

Figure (1): Workflow for Map Production from HRSI.

Figure (2): Image for the Study Area with GCPs.

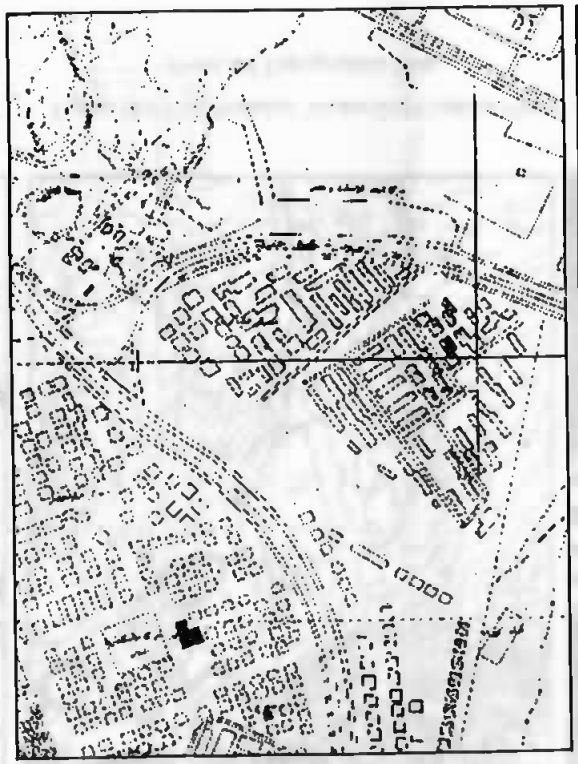

Figure (3): Cadastral Map for the Study Area.

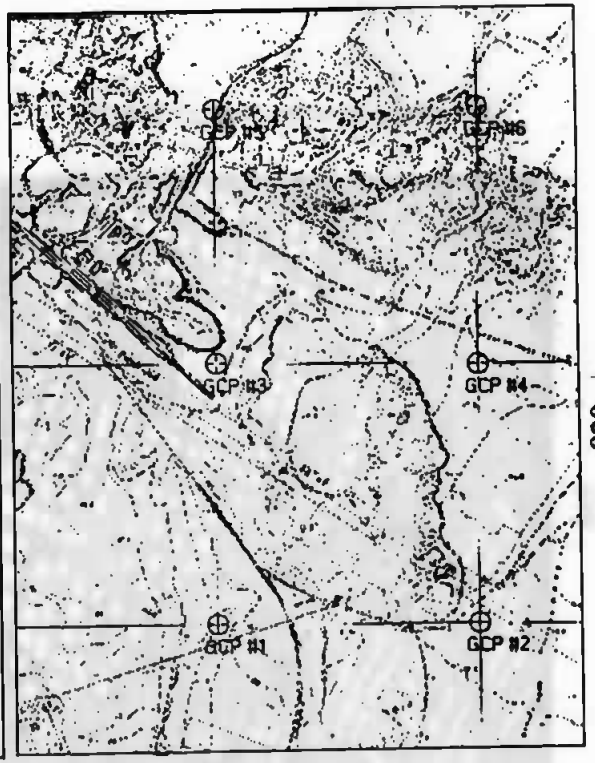

Figure (4): Topographic Map for the Study Area.

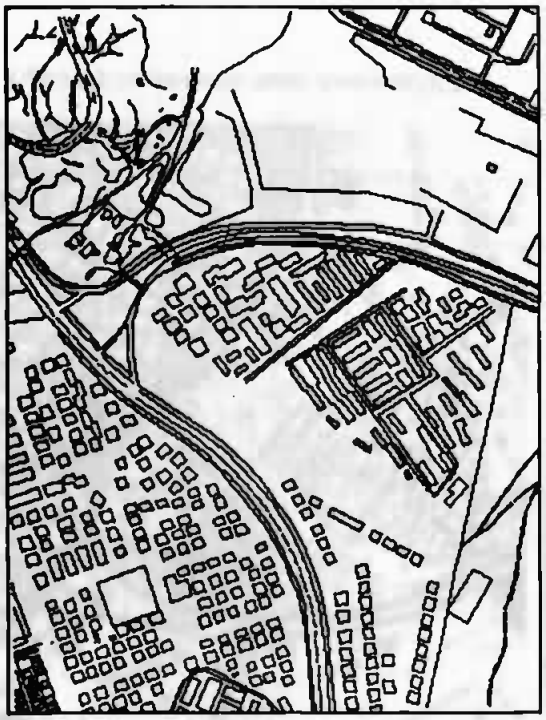

Figure (5): Vectorization of the Original Map Using Manual Digitizing.

Figure (6): The Produced Vectorized Contour Map From the Topographic Map.

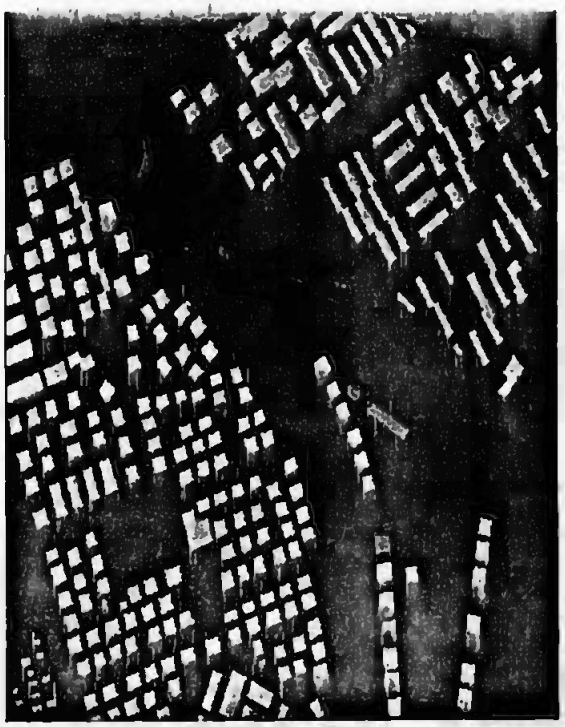

Figure (7): Created Digital Building Model.

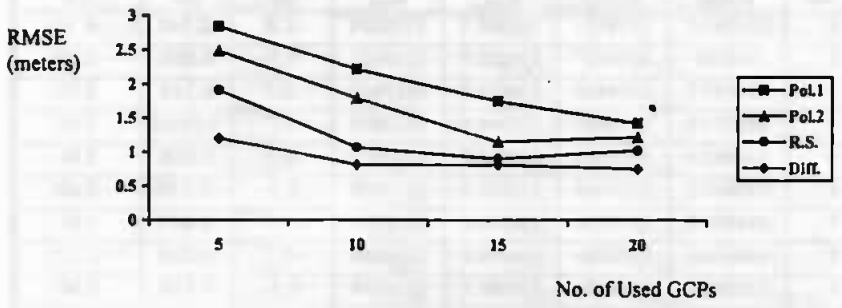

Figure (8): Graphical Representation of the RMSE of GCPs Control Points Using the Different Transformations Models.

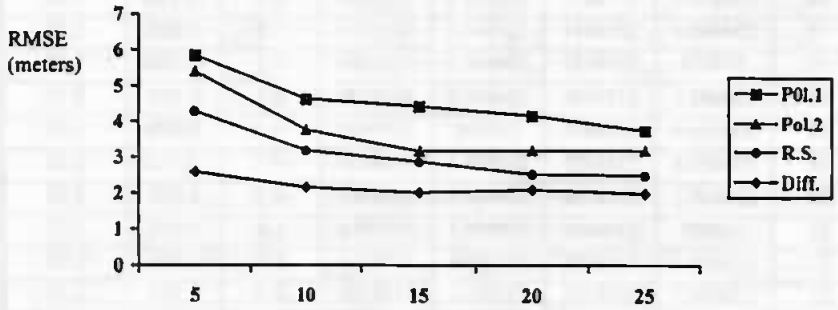

Figure (9): Graphical Representation of the RMSE of MRPs Using Different Transformations Models.

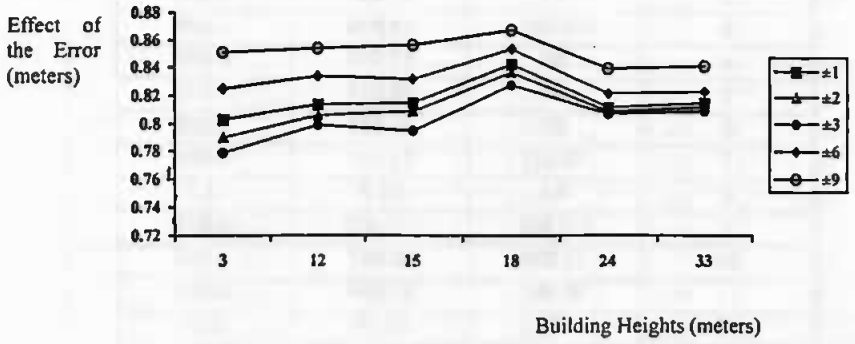

Fig (10) :Effect of the Error in Building Height Determination on the Horizontal Position of the Building, in meter.

Table (1): Checking the Planimetric Accuracy of the Base Map, in meters.

Pt. No.	E map	N map	E_{GPS}	N_{GPS}	ΔE	ΔN	ΔR
1	335263.5	3318521	335266.3	3318524	-2.8	-2.143	4.10
2	334624	3318437	334622.7	3318437	1.3	0.305	1.30
3	334617.5	3319450	334621.2	3319450	-3.7	0.748	3.70
4	335315.8	3319689	335314.1	3319692	1.7	1.7446	3.45
5	334963.5	3319024	334965.9	3319021	-2.4	2.555	3.84
6	335055.2	3319368	335052.8	3319368	2.4	-0.219	2.40
7	334902.7	3318734	334904.4	3318735	-1.7	-0.471	1.97
8	334456.2	3318986	334456.9	3318986	-0.7	-0.204	0.70
9	335282.2	3319076	335280.1	3319074	2.1	1.719	2.90
10	334870.1	3318357	334868.7	3318359	1.4	-1.751	2.44
11	335033.1	3319719	335031.9	3319723	1.2	-4.341	4.18
12	334744.6	3318999	334743.9	3318998	0.7	0.591	1.22
13	335223.1	3318852	335225	3318850	-1.9	2.298	2.76
14	334558.4	3318685	334558.2	3318686	0.2	-0.738	1.02
15	334548.4	3318314	334545.1	3318314	3.3	0.595	3.30
16	334850	3319382	334849.5	3319384	0.5	-1.395	2.06
17	334693.3	3319192	334693.2	3319192	0.1	0.108	0.10
18	335166.9	3319013	335168	3319010	-1.1	3.078	3.20
19	335031.6	3318437	335032.7	3318439	-1.1	-2.113	2.28
20	334445.7	3318582	334445.9	3318581	-0.2	1.325	1.02
21	334807	3319095	334805.2	3319094	1.8	0.458	2.06
22	335039.3	3319161	335039.4	3319159	-0.1	2.099	2.00
23	335054.7	3318791	335057.3	3318789	-2.6	2.197	3.28
24	335320.8	3319271	335322.3	3319268	-1.5	3.156	3.35
25	334755.3	3318465	334755.1	3318464	0.2	0.903	1.02

Table (2): Heights from DEM Versus those from Ordinary Leveling, in meters.

Point No.	DEM	O. Leveling	Difference
1	61.103	60.083	1.02
2	54	54.957	-0.957
3	72.267	74.615	-2.348
4	60	62.015	-2.015
5	65	66.015	-1.015
6	67	65.565	1.435
7	70.737	71.541	-0.804
8	64	66.7	-2.7
9	110.935	111.913	-0.978
10	51.098	52.667	-1.569
11	56.382	57.334	-0.952
12	57	59.29	-2.29
13	61.444	62.29	-0.846
14	70.79	72.762	-1.972
15	66.674	68.629	-1.955

Table (3): Statistics of the Differences between Measured (GCPs) and Transformed Coordinates at Using Different Transformation Models, in meters.

No. of GCPs	Statistics	Applied Mathematical Model			
		POL. 1	POL. 2	R. S.	Differential
5	Min.	0.126	0.485	0.218	0.565
	Max.	5.803	6.813	4.502	1.728
	Mean	2.378	2.583	1.465	1.089
	RMSE*	2.843	3.182	1.914	1.2
10	Min.	0.508	0.252	0.218	0.565
	Max.	4.038	3.565	3.622	2.116
	Mean	1.893	1.457	1.347	1.121
	RMSE*	2.219	1.787	1.064	0.816
15	Min.	0.092	0.273	0.218	0.565
	Max.	3.302	2.097	3.481	1.728
	Mean	1.52	1.002	1.313	1.007
	RMSE*	1.75	1.146	0.908	0.812
20	Min.	0.022	0.057	0.123	0.637
	Max.	2.491	2.813	1.77	1.225
	Mean	1.24	1.113	0.859	0.972
	RMSE*	1.425	1.417	1.03	0.753

Table (4): Statistics of the Differences among Measured (MRPs) and Transformed Coordinates at Using Different Transformation Models, in meters.

No. of MRPs	Statistics	Used Mathematical Model			
		POL. 1	POL. 2	R. S.	Differential
5	Min.	0.793	0.443	0.630	0.242
	Max.	12.815	9.080	8.987	5.498
	Mean	4.985	4.772	3.593	2.369
	RMSE*	5.863	5.405	4.297	2.594
10	Min.	0.515	1.018	0.130	0.432
	Max.	9.195	7.337	7.296	3.535
	Mean	3.724	3.801	2.678	2.035
	RMSE*	4.621	4.376	3.177	2.156
15	Min.	0.265	0.142	0.409	0.479
	Max.	8.072	6.752	7.219	3.410
	Mean	3.587	3.172	2.194	1.856
	RMSE*	4.442	3.710	2.873	2.024
20	Min.	1.093	0.375	0.309	1.315
	Max.	7.191	5.348	7.425	3.135
	Mean	3.837	3.177	1.932	2.006
	RMSE*	4.173	3.473	2.520	2.100
25	Min.	0.460	1.956	0.375	1.288
	Max.	8.628	4.172	3.694	3.298
	Mean	2.674	3.059	1.605	1.857
	RMSE*	3.743	3.164	1.973	1.998

Table (5): Statistics of the Differences between Measured (GCPs) and Transformed Coordinates at Using DBM and Different GCPs Configurations, in meters.

No. of GCPs	Statistics	Differences
5	Min.	0.247
	Max.	1.026
	Mean	0.790
	RMSE*	0.838
10	Min.	0.330
	Max.	1.214
	Mean	0.708
	RMSE*	0.764
15	Min.	0.323
	Max.	1.125
	Mean	0.615
	RMSE*	0.714
20	Min.	0.314
	Max.	1.093
	Mean	0.587
	RMSE*	0.702

Table (6): Accuracy of Orthorectification Process Using MRPs and DBM for Checkpoints.

Pt.	X image Pixel	Y image Pixel	E map meter	N map meter	Z map meter	ΔN meter	ΔE meter	ΔR meter
GCP8	589.625	-687.875	334963.45	3319023.9	18.00	-1.80	2.10	2.70
GCP 9	528.625	-949.875	334902.73	3318734.2	24.00	-0.70	-0.30	0.80
GCP 1	87.625	-715.375	334456.23	3318985.7	18.00	0.20	0.00	0.20
GCP 6	899.375	-640.375	335282.18	3319075.8	15.00	2.00	-1.30	2.40
GCP2	493.000	-1294.000	334870.11	3318357.1	24.00	0.30	-0.60	0.60
GCP 4	186.875	-991.375	334558.44	3318685.3	18.00	0.40	-0.50	0.70
GCP 3	173.000	-1333.000	334548.44	3318314.1	18.00	2.30	0.40	2.30
GCP 5	320.875	-527.625	334693.29	3319192.3	18.00	0.90	-0.80	1.20
GCP 7	679.625	-902.875	335054.70	3318791.0	3.00	-1.90	1.10	2.20
GCP10	785.000	-1198.000	335162.26	3318464.5	33.00	-1.90	-0.10	1.90

The Root Mean Square (RMS) error from the satellite modeling were 0.738 m and 1.743 m in E and Y respectively and the total RMS error were 1.893m.

Table (7) :Effect of the Error in Building Height Measurements on the Horizontal Position of the Building, in meter.

Error (m)	Building Height (meters)					
	3.00	12.00	15.00	18.00	24.00	33.00
±1	0.803	0.814	0.815	0.828	0.812	0.815
±2	0.790	0.806	0.809	0.827	0.809	0.812
±3	0.779	0.799	0.795	0.843	0.807	0.809
±6	0.825	0.834	0.832	0.854	0.822	0.823
±9	0.851	0.854	0.857	0.868	0.84	0.842